Supporting Information

Reversible on-off switching of Dy(III) single-molecule magnets via single-crystal-to-single-crystal transformation

Jing Xi,[a#] Peipei Cen,[b#] Yan Guo,[a#] Yuzhu Li,[a] Yuanyuan Qin,[a] Yi-Quan Zhang,*[,c] Weiming Song,[a] and Xiangyu Liu*[,a,d]

[a] State Key Laboratory of High-efficiency Utilization of Coal and Green Chemical Engineering, College of Chemistry and Chemical Engineering, Ningxia University, Yinchuan 750021, China

[b] College of Public Health and Management, Ningxia Medical University, Yinchuan 750021, China

[c] Jiangsu Key Laboratory for NSLSCS, School of Physical Science and Technology, Nanjing Normal University, Nanjing 210023, China

[d] State Key Laboratory of Coordination Chemistry, Nanjing University, Nanjing, 210023, China

# These authors contributed equally to this work.

***Corresponding author**

Dr. Xiangyu Liu

E-mail: xiangyuliu432@126.com

Prof. Yi-Quan Zhang

zhangyiquan@njnu.edu.cn

Contents

Table S1. Crystal Data and Structure Refinement Details for **1**, **2**, **2·CH_3CN**, **2-re and 2·CH_3CN-re**.

	1	**2**	**2·CH_3CN**	**2-re**	**2·CH_3CN-re**
Empirical formula	$C_{14}H_{12}Cl_5DyN_4$	$C_{32}H_{18}Cl_8DyN_7O_9$	$C_{33}H_{19.5}Cl_8DyN_{7.5}O_9$	$C_{32}H_{18}Cl_8DyN_7O_9$	$C_{33}H_{19.5}Cl_8DyN_{7.5}O_9$
Formula weight	576.03	1090.63	1111.16	1090.63	1111.16
Crystal system	monoclinic	monoclinic	triclinic	monoclinic	triclinic
Space group	*Cc*	$P2_1/n$	*P-1*	$P2_1/n$	*P-1*
a (Å)	7.1296(4)	12.0086(5)	11.2759(7)	12.212(14)	11.511(2)
b (Å)	21.1133(15)	16.5773(7)	13.1435(9)	17.002(19)	13.220(3)
c (Å)	13.1118(9)	20.2262(10)	15.0492(9)	20.87(3)	15.127(3)
α (°)	90	90	85.319(5)	90	81.914(7)
β (°)	91.917(6)	95.797(4)	68.224(6)	95.14(4)	68.257(6)
γ (°)	90	90	73.146(6)	90	72.685(6)
V (Å^3)	1972.6(2)	4005.8(3)	1981.4(2)	4315(9)	2040.2(8)
Z	4	4	2	4	2
μ (mm^{-1})	4.469	15.423	2.489	2.283	2.417
Unique reflections	2713	7881	9276	9589	9194
Observed reflections	4168	15315	18723	58946	70045
R_{int}	0.0386	0.0654	0.0430	0.0601	0.0350
Final R indices [I >2σ(I)]	R_1 = 0.0376	R_1 = 0.0905	R_1 = 0.0475	R_1 = 0.0602	R_1 = 0.0256
	wR_2 = 0.0783	wR_2 = 0.1821	wR_2 = 0.0842	wR_2 = 0.1097	wR_2 = 0.0594
R indices (all data)	R_1 = 0.0415	R_1 = 0.1127	R_1 = 0.0621	R_1 = 0.0963	R_1 = 0.0298
	wR_2 = 0.0822	wR_2 = 0.1925	wR_2 = 0.0915	wR_2 = 0.1262	wR_2 = 0.0619

Table S2. Selected bond lengths (Å) and bond angles (°) for **1**, **2**, **2·CH_3CN**, **2-re and 2·CH_3CN-re**.

Complex **1**			
Dy(1)-Cl(3)	2.618(4)	N(3)-Dy(1)-Cl(4)	85.7(3)
Dy(1)-Cl(4)	2.629(3)	N(3)-Dy(1)-Cl(5)	84.3(3)
Dy(1)-Cl(5)	2.603(3)	N(3)-Dy(1)-N(1)	127.7(4)
Dy(1)-N(1)	2.609(11)	N(3)-Dy(1)-N(2)	65.6(3)
Dy(1)-N(2)	2.480(10)	N(3)-Dy(1)-N(4)	64.9(4)
Dy(1)-N(3)	2.464(11)	N(4)-Dy(1)-Cl(3)	83.8(3)
Dy(1)-N(4)	2.552(12)	N(4)-Dy(1)-Cl(4)	87.6(2)
Cl(3)-Dy(1)-Cl(4)	92.53(10)	N(4)-Dy(1)-Cl(5)	89.9(2)
Cl(5)-Dy(1)-Cl(3)	97.08(10)	N(4)-Dy(1)- N(1)	166.7(4)
Cl(5)-Dy(1)-Cl(4)	169.75(11)	C(1)-N(1)- Dy(1)	125.0(9)
Cl(1)-Dy(1)- N(1)	87.3(2)	C(5)-N(1)- Dy(1)	117.6(9)
N(1)-Dy(1)-Cl(3)	83.7(3)	C(6)-N(2)- Dy(1)	122.1(9)
N(1)-Dy(1)-Cl(4)	97.3(2)	C(7)-N(2)- Dy(1)	118.2(7)
N(2)-Dy(1)-Cl(3)	144.6(2)	C(8)-N(3)- Dy(1)	119.0(8)
N(2)-Dy(1)-Cl(4)	79.1(2)	C(9)-N(3)- Dy(1)	121.2(9)
N(2)-Dy(1)-Cl(5)	94.9(2)	C(10)-N(4)- Dy(1)	117.8(9)
N(2)-Dy(1)-N(1)	63.8(3)	C(14)-N(4)- Dy(1)	126.7(9)
N(2)-Dy(1)- N(4)	129.5(4)	C(48)-N(2)- Dy(1)	122.1(4)
N(3)-Dy(1)-Cl(3)	148.6(3)	C(52)-N(2)- Dy(1)	120.3(3)

Complex **2**			
Dy(1)-O(1)	2.171(7)	O(4)-Dy(1)-N(2)	150.2(3)
Dy(1)-O(4)	2.175(7)	O(4)-Dy(1)-N(3)	144.2(3)
Dy(1)-O(7)	2.180(8)	O(4)-Dy(1)-N(4)	80.9(3)
Dy(1)-N(1)	2.531(9)	O(7)-Dy(1)-N(1)	86.8(3)
Dy(1)-N(2)	2.486(9)	O(7)-Dy(1)-N(2)	86.2(4)
Dy(1)-N(3)	2.479(9)	O(7)-Dy(1)-N(3)	81.9(3)
Dy(1)-N(4)	2.558(9)	O(7)-Dy(1)-N(4)	99.4(3)
O(1)-Dy(1)- O(4)	98.0(3)	N(1)-Dy(1)-N(4)	165.2(3)
O(1)-Dy(1)- O(7)	164.6(3)	N(2)-Dy(1)-N(1)	65.0(3)
O(1)-Dy(1)- N(1)	86.3(3)	N(2)-Dy(1)-N(4)	128.4(3)
O(1)-Dy(1)- N(2)	78.4(3)	N(3)-Dy(1)-N(1)	129.8(3)
O(1)-Dy(1)- N(3)	92.1(3)	N(3)-Dy(1)-N(2)	65.5(3)
O(1)-Dy(1)- N(4)	90.6(3)	N(3)-Dy(1)-N(4)	64.7(3)
O(4)-Dy(1)- O(7)	95.1(3)	C(15)-O(1)-Dy(1)	178.2(7)
O(4)-Dy(1)- N(1)	85.3(3)	C(21)-O(4)-Dy(1)	164.1(15)

Complex **2·CH$_3$CN**			
Dy(1)-O(1)	2.201(3)	O(7)-Dy(1)-N(3)	89.25(12)
Dy(1)-O(4)	2.210(3)	O(7)-Dy(1)-N(4)	90.87(12)
Dy(1)-O(7)	2.180(3)	N(2)-Dy(1)-N(1)	65.15(12)
Dy(1)-N(1)	2.549(4)	N(2)-Dy(1)-N(3)	65.11(13)
Dy(1)-N(2)	2.494(4)	N(2)-Dy(1)-N(4)	128.74(13)
Dy(1)-N(3)	2.496(4)	N(3)-Dy(1)-N(1)	127.28(12)
Dy(1)-N(4)	2.548(4)	N(3)-Dy(1)-N(4)	64.74(12)
O(1)-Dy(1)-O(4)	97.51(11)	N(4)-Dy(1)-N(1)	165.41(12)
O(1)-Dy(1)- N(1)	85.50(12)	C(15)-O(1)-Dy(1)	168.2(3)
O(1)-Dy(1)- N(2)	148.84(13)	C(21)-O(4)-Dy(1)	151.4(3)
O(1)-Dy(1)- N(3)	145.98(13)	C(27)-O(7)-Dy(1)	168.2(3)
O(1)-Dy(1)-N(4)	81.54(12)	C(1)-N(1)-Dy(1)	125.5(3)
O(4)-Dy(1)-N(1)	85.31(11)	C(5)-N(1)-Dy(1)	117.0(3)
O(4)-Dy(1) N(2)	90.56(11)	C(6)-N(2)-Dy(1)	120.5(3)
O(4)-Dy(1)-N(3)	78.81(12)	C(7)-N(2)-Dy(1)	119.0(3)
O(4)-Dy(1)-N(4)	89.76(12)	C(8)-N(3)-Dy(1)	119.2(3)
O(7)-Dy(1)-O(1)	95.95(12)	C(9)-N(3)-Dy(1)	121.6(3)
O(7)-Dy(1)-O(4)	166.47(12)	C(10)-N(4)-Dy(1)	118.2(3)
O(7)-Dy(1)-N(1)	97.13(12)	C(14)-N(4)-Dy(1)	124.8(3)
O(7)-Dy(1)-N(2)	78.53(11)	C(14)-N(4)-C(10)	116.8(4)

Complex **2-re**			
Dy(1)-O(1)	2.218(5)	O(7)-Dy(1)-N(3)	78.59(7)
Dy(1)-O(4)	2.218(5)	O(7)-Dy(1)-N(6)	79.1(2)
Dy(1)-O(7)	2.206(5)	O(7)-Dy(1)-N(7)	88.24(19)
Dy(1)-N(4)	2.596(6)	N(5)-Dy(1)-N(4)	64.0(2)
Dy(1)-N(5)	2.548(6)	N(5)-Dy(1)-N(7)	129.6(2)
Dy(1)-N(6)	2.529(6)	N(6)-Dy(1)-N(4)	127.6(2)
Dy(1)-N(7)	2.577(6)	N(6)-Dy(1)-N(5)	65.0(2)
O(1)-Dy(1)-O(4)	95.4(2)	N(6)-Dy(1)-N(7)	65.4(2)
O(1)-Dy(1)- N(4)	97.7(2)	N(7)-Dy(1)-N(4)	166.37(19)
O(1)-Dy(1)- N(5)	82.25(19)	C(1)-O(1)-Dy(1)	162.0(8)
O(1)-Dy(1)- N(6)	86.7(2)	C(7)-O(4)-Dy(1)	177.3(9)
O(1)-Dy(1)-N(7)	86.62(19)	C(13)-O(7)-Dy(1)	177.8(5)
O(4)-Dy(1)-N(4)	81.9(2)	C(19)-N(4)-Dy(1)	124.3(5)
O(4)-Dy(1) N(5)	145.0(2)	C(23)-N(4)-Dy(1)	117.9(5)
O(4)-Dy(1)-N(6)	150.0(2)	C(24)-N(5)-Dy(1)	121.8(5)
O(4)-Dy(1)-N(7)	84.8(2)	C(26)-N(6)-Dy(1)	118.0(5)
O(7)-Dy(1)-O(1)	165.80(19)	C(27)-N(6)-Dy(1)	119.5(5)
O(7)-Dy(1)-O(4)	97.3(2)	C(28)-N(7)-Dy(1)	117.7(4)
O(7)-Dy(1)-N(4)	90.3(2)	C(32)-N(7)-Dy(1)	125.2(5)
O(7)-Dy(1)-N(5)	90.9(2)	C(32)-N(7)-C(28)	117.1(6)

Complex **2·CH_3CN-re**			
Dy(1)-O(1)	2.181(2)	O(7)-Dy(1)-N(3)	78.59(7)
Dy(1)-O(4)	2.1910(18)	O(7)-Dy(1)-N(4)	89.84(8)
Dy(1)-O(7)	2.2135(18)	N(1)-Dy(1)-N(2)	64.44(7)
Dy(1)-N(1)	2.564(2)	N(2)-Dy(1)-N(3)	65.41(7)
Dy(1)-N(2)	2.501(2)	N(2)-Dy(1)-N(4)	129.00(7)
Dy(1)-N(3)	2.505(2)	N(3)-Dy(1)-N(1)	126.75(7)
Dy(1)-N(4)	2.553(2)	N(3)-Dy(1)-N(4)	64.56(7)
O(1)-Dy(1)-O(4)	96.67(8)	N(4)-Dy(1)-N(1)	165.47(7)
O(1)-Dy(1)- O(7)	164.85(7)	C(15)-O(1)-Dy(1)	166.9(2)
O(1)-Dy(1)- N(1)	98.69(8)	C(21)-O(4)-Dy(1)	171.02(18)
O(1)-Dy(1)- N(2)	78.47(8)	C(27)-O(7)-Dy(1)	157.2(4)
O(1)-Dy(1)-N(3)	87.83(8)	C(1)-N(1)-Dy(1)	125.12(18)
O(1)-Dy(1)-N(4)	90.37(8)	C(5)-N(1)-Dy(1)	117.54(17)
O(4)-Dy(1) O(7)	98.36(7)	C(6)-N(1)-Dy(1)	121.48(18)
O(4)-Dy(1)-N(1)	85.78(7)	C(7)-N(2)-Dy(1)	118.07(17)
O(4)-Dy(1)-N(2)	148.30(7)	C(8)-N(3)-Dy(1)	118.85(17)
O(4)-Dy(1)-N(3)	146.21(8)	C(9)-N(3)-Dy(1)	121.18(18)
O(4)-Dy(1)-N(4)	81.89(7)	C(10)-N(4)-Dy(1)	118.10(18)
O(7)-Dy(1)-N(1)	84.37(7)	C(14)-N(4)-Dy(1)	124.75(18)
O(7)-Dy(1)-N(2)	89.67(7)	C(14)-N(4)-C(10)	117.0(2)

Table S3. Dy (III) ions geometry analysis of **1**, **2** and **2·CH$_3$CN** by SHAPE 2.1 software.

Dy (III) ion geometry analysis of **1**

PBPY-7	3 D5h	Pentagonal bipyramid
COC-7	4 C3v	Capped octahedron
CTPR-7	5 C2v	Capped trigonal prism
JPBPY-7	6 D5h	Johnson pentagonal bipyramid J13
JETPY-7	7 C3v	Johnson elongated triangular pyramid J7

Structure [ML7]	PBPY-7	COC-7	CTPR-7	JPBPY-7	JETPY-7
ABOXIY ,	1.407,	6.082,	4.636,	5.560,	22.819

Dy (III) ion geometry analysis of **2**

PBPY-7	3 D5h	Pentagonal bipyramid
COC-7	4 C3v	Capped octahedron
CTPR-7	5 C2v	Capped trigonal prism
JPBPY-7	6 D5h	Johnson pentagonal bipyramid J13
JETPY-7	7 C3v	Johnson elongated triangular pyramid J7

Structure [ML7]	PBPY-7	COC-7	CTPR-7	JPBPY-7	JETPY-7
ABOXIY ,	1.401,	6.090,	4.720,	3.075,	22.753

Dy (III) ion geometry analysis of **2·CH$_3$CN**

PBPY-7	3 D5h	Pentagonal bipyramid
COC-7	4 C3v	Capped octahedron
CTPR-7	5 C2v	Capped trigonal prism
JPBPY-7	6 D5h	Johnson pentagonal bipyramid J13
JETPY-7	7 C3v	Johnson elongated triangular pyramid J7

Structure [ML7]	PBPY-7	COC-7	CTPR-7	JPBPY-7	JETPY-7
ABOXIY ,	1.431,	6.046,	4.848,	3.238,	22.405

Configuration	ABOXIY, **1**	ABOXIY, **2**	ABOXIY, **2·CH$_3$CN**
Pentagonal bipyramid (D_{5h})	**1.407**	**1.401**	**1.431**
Capped octahedron (C_{3v})	6.082	6.096	6.046
Capped trigonal prism (C_{2v})	4.636	4.720	4.848
Johnson pentagonal bipyramid J13 (D_{5h})	5.560	3.075	3.238
Johnson elongated triangular pyramid J7 (C_{3v})	22.819	22.753	22.405

Table S4. Relaxation fitting parameters from least-squares fitting of $\chi(f)$ data under 500 Oe dc field of **1**.

T(K)	χ_T	χ_S	α
2.0	2.775	1.278	0.135
2.2	2.596	1.177	0.130
2.4	2.439	1.093	0.121
2.6	2.293	1.002	0.120
2.8	2.161	0.845	0.134
3.0	2.045	0.112	0.187
3.2	1.934	0.020	0.157
3.4	1.836	0.035	0.163
3.6	1.746	0.051	0.159

Table S5. Relaxation fitting parameters from least-squares fitting of $\chi(f)$ data under 1000 Oe dc field of **2**.

T(K)	χ_T	χ_S	α
2.0	5.599	0.127	0.625
2.5	3.486	0.252	0.489
3.0	2.794	0.293	0.436
3.5	2.269	0.383	0.313
4.0	1.937	0.403	0.213
4.5	1.709	0.383	0.154
5.0	1.539	0.355	0.118
5.5	1.400	0.332	0.088
6.0	1.283	0.312	0.069
6.5	1.186	0.293	0.058
7.0	1.102	0.280	0.046
7.5	1.029	0.267	0.039
8.0	0.966	0.256	0.034
8.5	0.909	0.247	0.027
9.0	0.859	0.235	0.023
9.5	0.816	0.208	0.032

Table S6. Relaxation fitting parameters from least-squares fitting of $\chi(f)$ data under zero dc field of **2·CH$_3$CN**.

T(K)	χ_T	χ_S	α
3.0	2.294	0.129	0.184
4.0	1.715	0.104	0.182
5.0	1.370	0.087	0.181
6.0	1.140	0.076	0.178
6.5	1.051	0.072	0.175
7.0	0.976	0.069	0.171
7.5	0.910	0.066	0.165
8.0	0.853	0.064	0.159
8.5	0.802	0.062	0.151
9.0	0.757	0.061	0.142
9.5	0.716	0.060	0.132
10.0	0.680	0.059	0.121
10.5	0.647	0.058	0.110
11.0	0.618	0.057	0.100
11.5	0.590	0.056	0.089
12.0	0.565	0.055	0.079
12.5	0.542	0.054	0.070
13.0	0.521	0.053	0.061
13.5	0.502	0.053	0.053
14.0	0.484	0.052	0.046
15.0	0.452	0.051	0.034
16.5	0.425	0.051	0.025
17.0	0.400	0.050	0.019
18.0	0.378	0.049	0.015

Table S7. Wave functions with definite projection of the total moment | m_J > for the lowest two KDs of individual Dy^{III} fragments for complexes **1**, **2** and **2·CH$_3$CN** using CASSCF/RASSI with MOLCAS 8.4.

	E	wave functions
1	0.0	95.4%|±15/2>
	71.5	34.3%|±1/2>+24.3%|±3/2>+16.7%|±5/2>+8.6%|±7/2>+5.7%|±9/2>
2	0.0	98.7%|±15/2>
	163.1	37.5%|±1/2>+25.5%|±3/2>+15.8%|±5/2>+7.4%|±7/2>+5.4%|±13/2>
2·CH$_3$CN	0.0	98.8%|±15/2>
	224.7	27.1%|±1/2>+21%|±13/2>+18.4%|±3/2>+14.1%|±5/2>+7.6%|±7/2>+6.9%|±9/2>

Table S8. Calculated energy levels (cm^{-1}), ***g*** (g_x, g_y, g_z) tensors and predominant m_J values of the lowest eight Kramers doublets (KDs) of complexes **1**, **2** and **2·CH$_3$CN** using CASSCF/RASSI-SO with MOLCAS 8.4.

KDs	**1**			**2**			**2·CH$_3$CN**		
	E	***g***	m_J	*E*	***g***	m_J	*E*	***g***	m_J
1	0.0	0.268 0.810 19.233	±15/2	0.0	0.082 0.180 19.725	±15/2	0.0	0.051 0.097 19.759	±15/2
2	71.5	0.256 0.956 18.186	±1/2	163.1	0.772 0.872 18.756	±1/2	224.7	1.355 2.941 16.613	±9/2
3	205.3	3.579 4.515 11.867	±13/2	306.6	1.852 2.767 13.965	±13/2	318.4	0.279 3.290 11.813	±13/2
4	271.2	9.311 6.632 0.762	±7/2	422.4	1.355 5.369 11.546	±5/2	467.2	9.083 6.522 3.550	±11/2
5	303.2	2.303 5.119 12.719	±9/2	479.0	3.073 5.028 12.667	±11/2	527.2	0.946 4.249 14.000	±5/2
6	322.8	0.215 1.118 14.030	±11/2	513.6	0.542 1.547 15.155	±9/2	574.1	0.703 2.763 14.387	±3/2
7	379.9	0.449 0.732 14.587	±5/2	567.4	0.843 1.444 14.647	±3/2	632.4	0.874 1.400 15.849	±1/2
8	453.1	0.118 0.271 18.258	±3/2	641.9	0.499 0.772 17.910	±7/2	708.9	0.271 0.625 18.048	±7/2

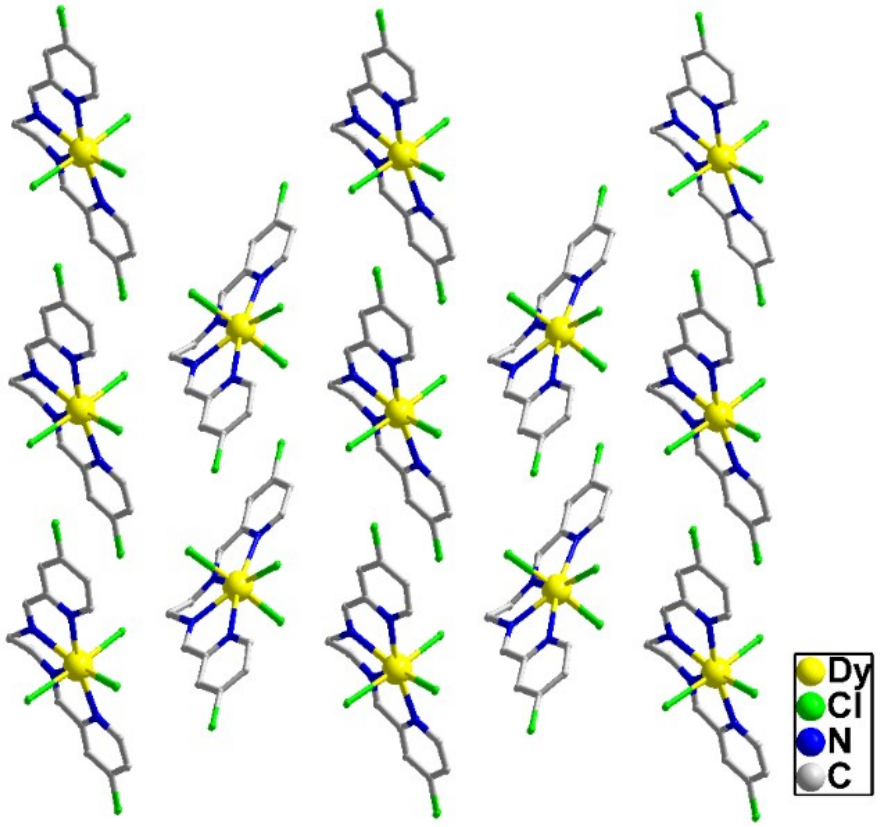

Fig. S1 Crystal packing diagram for complex **1**.

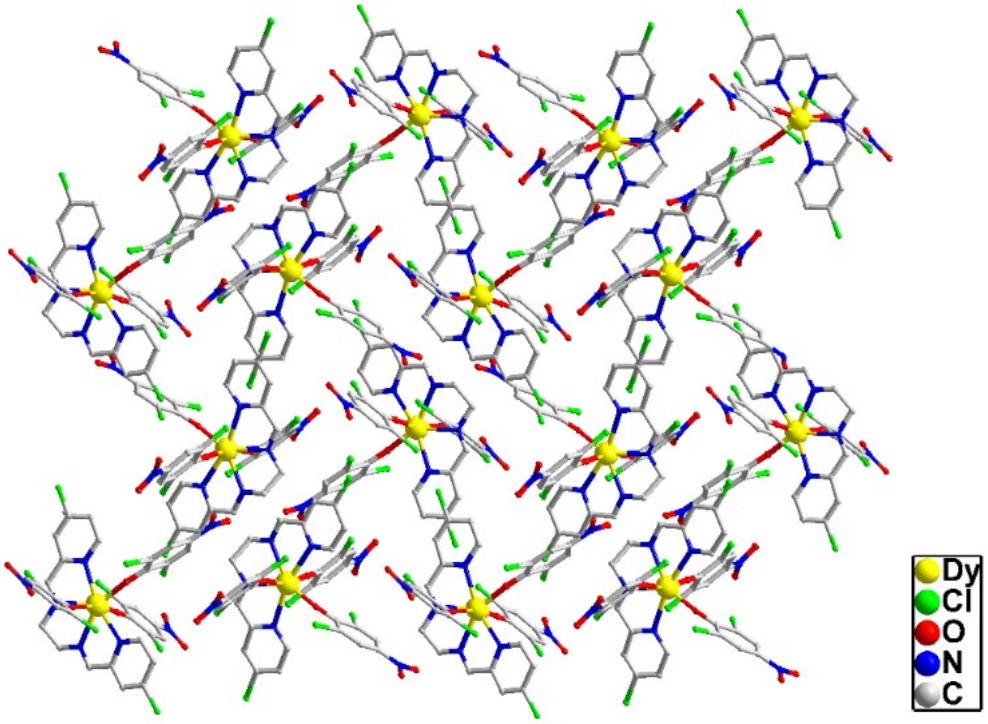

Fig. S2 Crystal packing diagram for complex **2**.

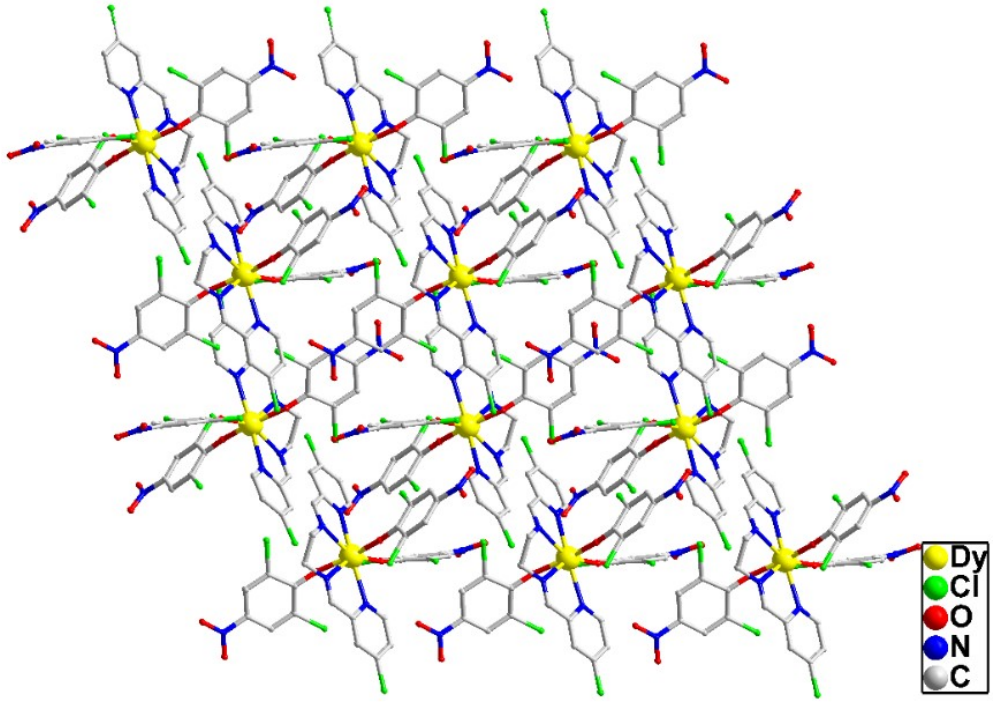

Fig. S3 Crystal packing diagram for complex **2·CH$_3$CN**.

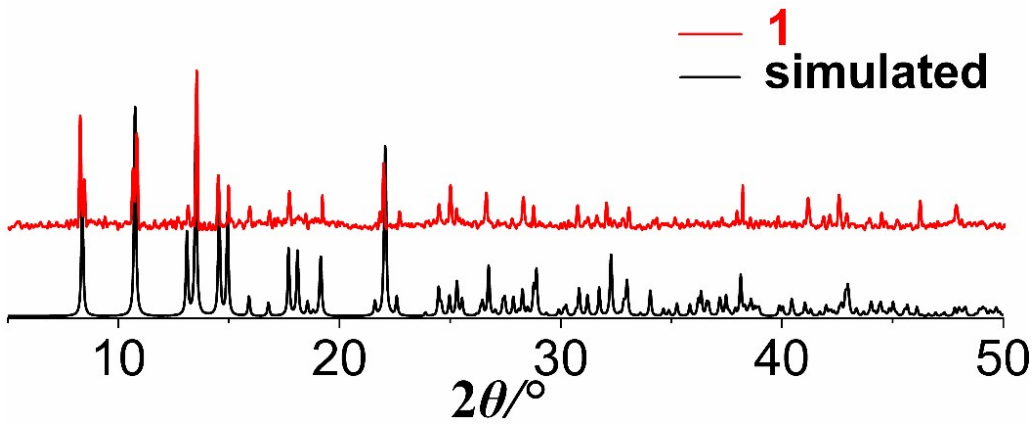

Fig. S4 Powder XRD patterns for complex **1**.

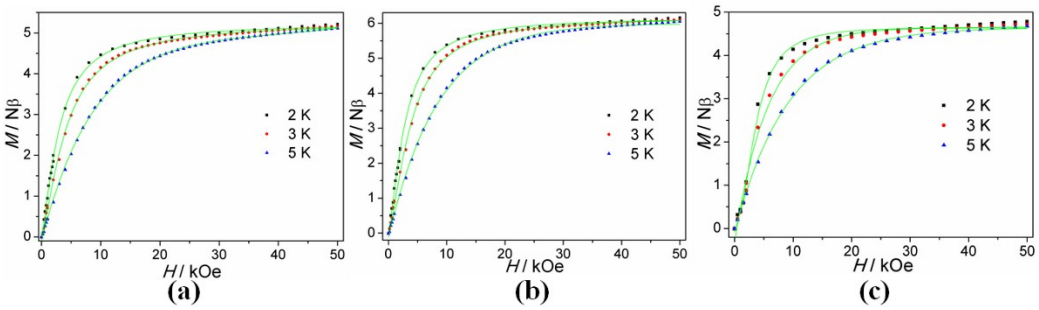

Fig. S5 *M* vs *H* curves for **1** (a), **2** (b) and **2·CH$_3$CN** (c) at different temperatures. Solid lines represent the simulation from *ab initio* calculation.

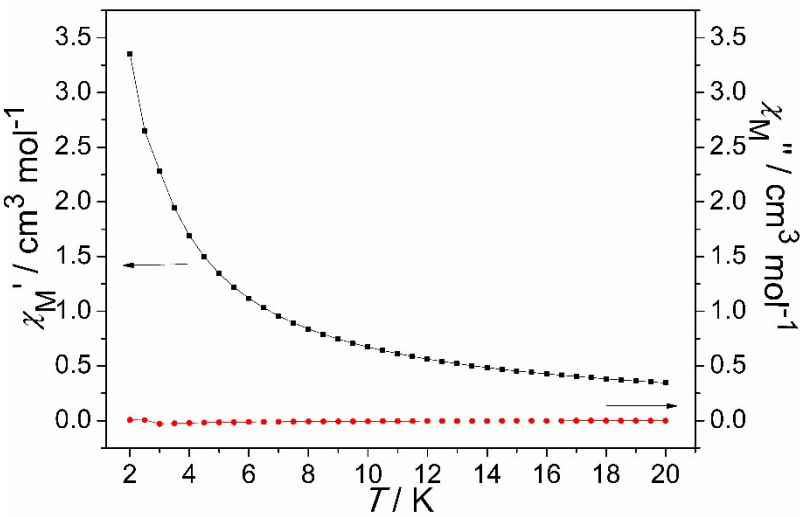

Fig. S6 Temperature dependence of χ' and χ'' susceptibilities for **1** without static field.

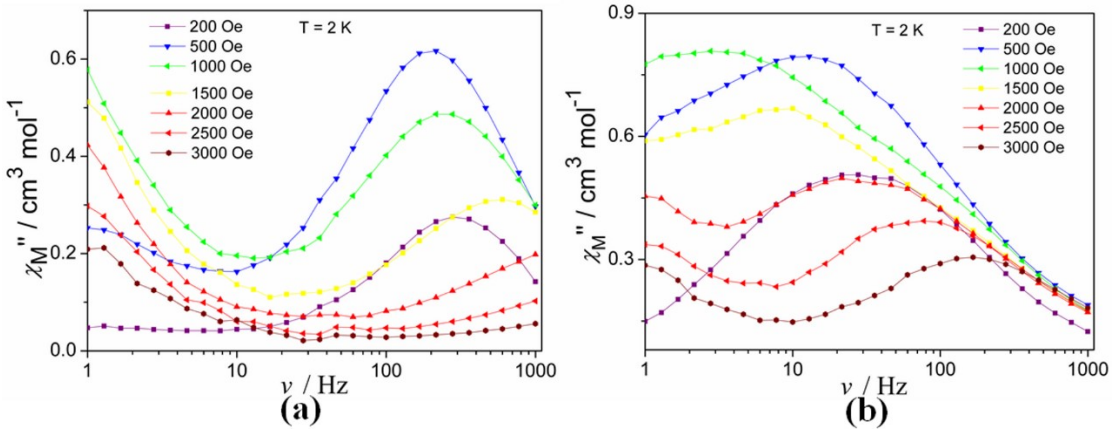

Fig. S7 The χ'' products for **1** and **2** at 2.0 K under different static fields

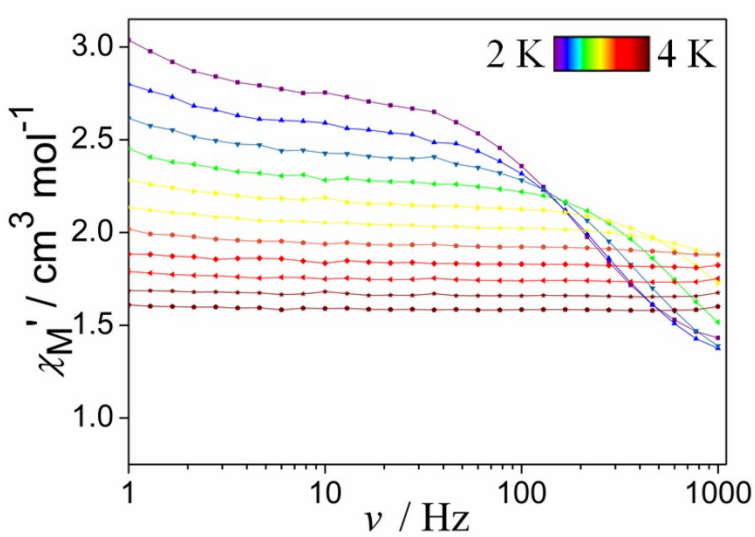

Fig. S8 Frequency dependence of χ' susceptibilities for **1** at applied dc fields of 500 Oe.

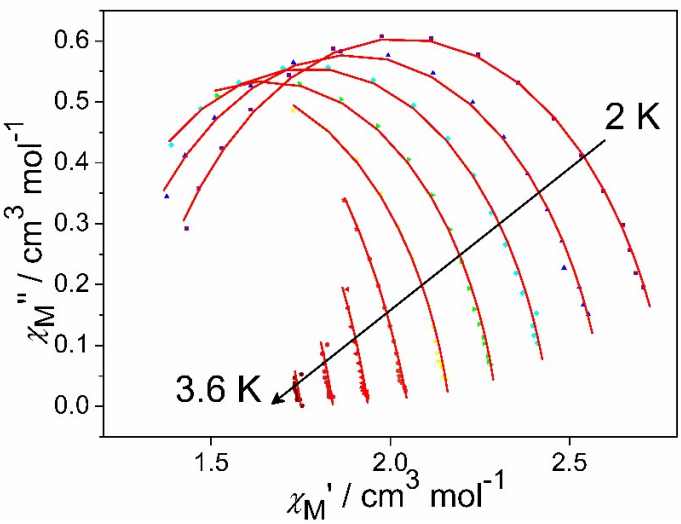

Fig. S9 Cole-Cole plots for **1** at applied dc fields of 500 Oe. The solid lines represent the best fit to the measured results.

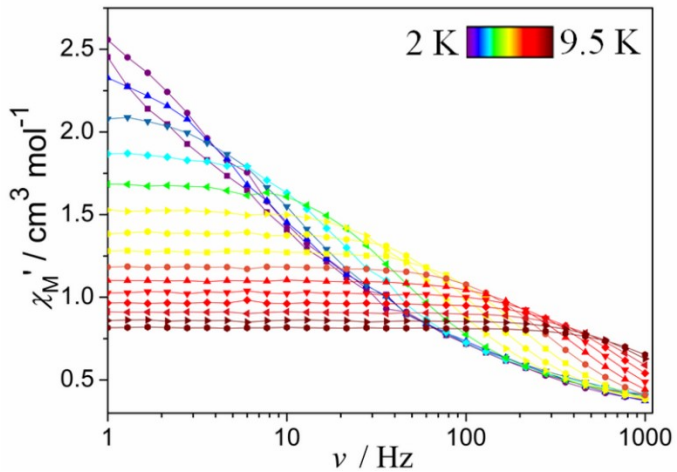

Fig. S10 Frequency dependence of χ' susceptibilities for **2** at applied dc fields of 1000 Oe.

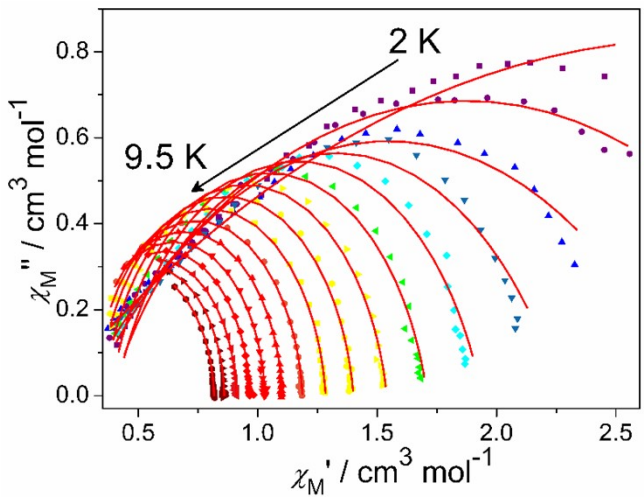

Fig. S11 Cole-Cole plots for **2** at applied dc fields of 1000 Oe. The solid lines represent the best fit to the measured results

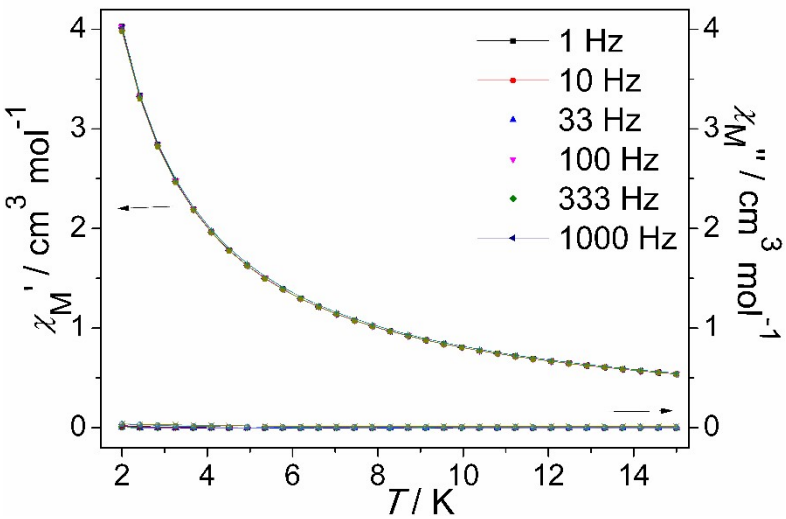

Fig. S12 Temperature dependence of χ' and χ'' susceptibilities for **2-re** without static field.

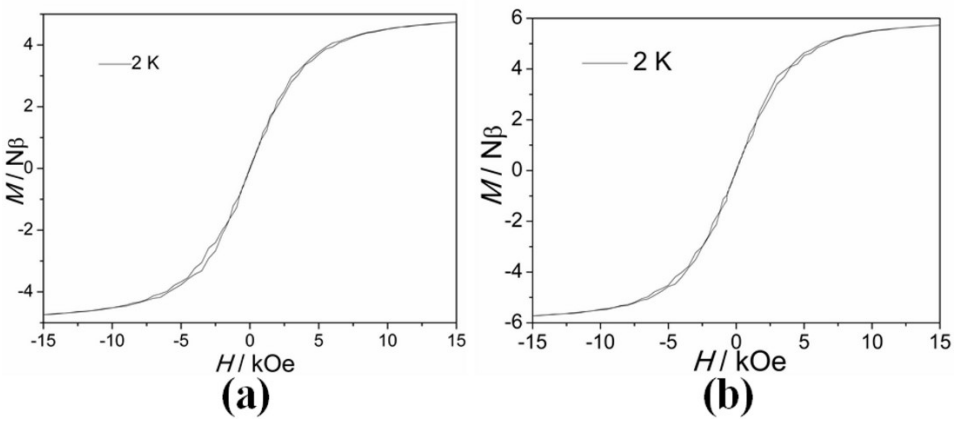

Fig. S13 Magnetic hysteresis loops for **1** (a) and **2** (b).

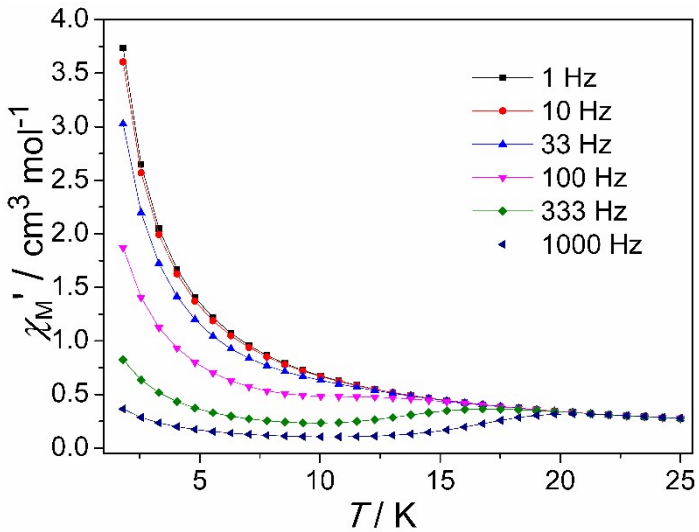

Fig. S14 Temperature dependence of χ' susceptibilities for **2·CH$_3$CN** without static field.

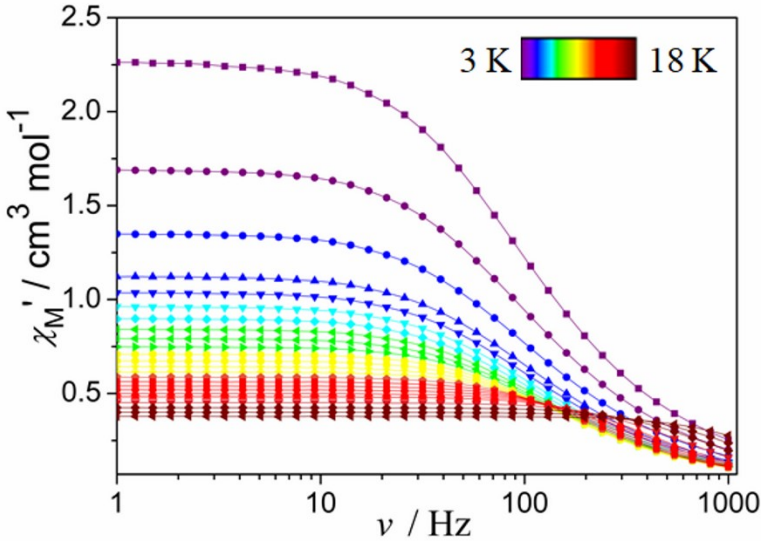

Fig. S15 Frequency dependence of χ' susceptibilities for **2·CH$_3$CN** without static field.